MICROBIOLOGY

Bacteriology | Full-Length Text

Myxococcus xanthus PilB interacts with c-di-GMP and modulates motility and biofilm formation

Keane J. Dye, ¹ Safoura Salar, ¹ Uvina Allen, ¹ Wraylyn Smith, ¹ Zhaomin Yang ¹

AUTHOR AFFILIATION See affiliation list on p. 13.

ABSTRACT The regulation of biofilm and motile states as alternate bacterial lifestyles has been studied extensively in flagellated bacteria, where the second messenger cyclic-di-GMP (cdG) plays a crucial role. However, much less is known about the mechanisms of such regulation in motile bacteria without flagella. The bacterial type IV pilus (T4P) serves as a motility apparatus that enables Myxococcus xanthus to move on solid surfaces. PilB, the T4P assembly ATPase, is, therefore, required for T4P-dependent motility in M. xanthus. Interestingly, T4P is also involved in the regulation of exopolysaccharide as the biofilm matrix material in this bacterium. A newly discovered cdG-binding domain, MshE_N, is conserved in the N-terminus of PilB (PilB_N) in M. xanthus and other bacteria. This suggests that cdG may bind to PilB to control the respective outputs that regulate biofilm development and T4P-powered motility. In this study, we aimed to validate M. xanthus PilB as a cdG effector protein. We performed a systematic mutational analysis of its cdG-binding domain to investigate its relationship with motility, piliation, and biofilm formation. Excluding those resulting in low levels of PilB protein, all other substitution mutations in PilB_N resulted in pilB mutants with distinct and differential phenotypes in piliation and biofilm levels in M. xanthus. This suggests that the PilB_N domain plays dual roles in modulating motility and biofilm levels, and these two functions of PilB can be dependent on and independent of each other in M. xanthus.

IMPORTANCE The regulation of motility and biofilm by cyclic-di-GMP in flagellated bacteria has been extensively investigated. However, our knowledge regarding this regulation in motile bacteria without flagella remains limited. Here, we aimed to address this gap by investigating a non-flagellated bacterium with motility powered by bacterial type-IV pilus (T4P). Previous studies hinted at the possibility of *Myxococcus xanthus* PilB, the T4P assembly ATPase, serving as a cyclic-di-GMP effector involved in regulating both motility and biofilm. Our findings strongly support the hypothesis that PilB directly interacts with cyclic-di-GMP to act as a potential switch to promote biofilm formation or T4P-dependent motility. These results shed light on the bifurcation of PilB functions and its pivotal role in coordinating biofilm formation and T4P-mediated motility.

KEYWORDS cyclic-di-GMP, PilB ATPase, type IV pilus (T4P), biofilm, motility

n the natural environment, bacteria predominantly exist in either a planktonic/motile or a biofilm/sessile state (1, 2). Bacteria in the planktonic state are typically individual cells that often display some form of motility, like that powered by flagellar rotation (3–6). Those in the biofilm state are typically non-motile, forming surface-associated multicellular communities often encased in self-produced exopolysaccharide (EPS) as the biofilm matrix (7). Bacteria actively alternate between these two states or lifestyles depending on physiochemical properties of their surrounding environment (1, 8–10). Environmental cues, processed through a multitude of signal transduction pathways (11), may converge on or translate into the regulation of the second messenger

Editor Michael Y. Galperin, NCBI, NLM, National Institutes of Health, Bethesda, Maryland, USA

Address correspondence to Zhaomin Yang, zmvang@vt.edu.

The authors declare no conflict of interest.

See the funding table on p. 13.

Received 9 July 2023 Accepted 2 August 2023 Published 11 September 2023

Copyright © 2023 American Society for Microbiology. All Rights Reserved.

Downloaded from https://journals.asm.org/journal/jb on 11 September 2023 by 2001:468:c80:610b:b9c3:185c:cd77:cce1

cyclic-di-GMP (c-di-GMP or cdG) inside the cell (12, 13). The levels of cdG are crucial in the lifestyle choices of bacteria as has been revealed by extensive investigation in flagellated bacteria (12, 14). The established paradigm is that low levels of cdG favor the motile state and inhibit biofilm formation while high levels do the opposite (11–13).

The effects of cdG on bacterial lifestyles are exercised through its binding to cdG effectors, which include regulatory proteins, enzymes, and regulatory RNAs (12, 14). These effectors, in turn, directly or indirectly regulate the choice of one lifestyle over the other at transcriptional, posttranscriptional, and posttranslational levels (10, 12, 13). The functioning of the flagellar motor, for example, can be inhibited posttranslationally by cdG effectors YcgR in Escherichia coli, Motl in Bacillus subtilis, and PlzD in Vibrio cholerae (15-18). The inhibition of motility generally coincides with increased EPS production mediated by other effectors to complete the switching from a motile to a biofilm state in these flagellated bacteria (19, 20). For instance, the binding of cdG to the transcriptional regulators VpsT and VpsR leads to transcriptional activation of genes for the production of EPS and other biofilm matrix materials in V. cholerae (18).

The retractable bacterial type IV pilus (T4P) (21) is a motility apparatus with dual functions in motility and biofilm formation (22-26). It is known to power bacterial surface locomotion through recurrent cycles of extension and retraction by a "grappling hook" mechanism (27, 28). This form of motility is known as twitching in most bacteria and social (S) motility in Myxococcus xanthus (29-32). The most convenient assay for M. xanthus S motility is the macroscopic measurement of colony expansion on soft agar plates (with ≤0.5% agar). This is because M. xanthus adventurous (A) gliding motility, while effective in driving colony expansion on hard agar plates (with ≥1.5% agar), does not do so on soft agar surfaces (31, 33). Interestingly, it is well established that the presence of T4P stimulates the production of EPS in M. xanthus, and T4P-deficient mutants (T4P⁻) exhibit minimal to no production of this crucial biofilm matrix (34–38). . It was observed more recently that M. xanthus EPS, but not its T4P, is crucial for the formation of submerged biofilms in this bacterium (39). Of particular importance here is the T4P assembly ATPase PilB (40). It possesses a signaling function in EPS regulation, and this function can be decoupled from its role in T4P assembly by genetic mutations (40). The dual roles of T4P in promoting both motility and biofilm formation in M. xanthus are somewhat paradoxical because motility is most often associated with the planktonic lifestyle and sessility with biofilms.

Recent studies suggested that cdG could impact the function of T4P in motility and biofilm formation. Significant increases in the concentration of cdG in M. xanthus was found to inhibit S motility and bacterial agglutination, a phenomenon functionally related to EPS levels (41). This inhibition coincides with reduced piliation levels, showing that cdG can impact T4P biogenesis and possibly EPS production. SgmT is a cdG-binding protein with regulatory roles in S motility and EPS production (42). A systematic analysis of PilZ domain-encoding genes identified pixA, pixB, and plpA (43) as important for S motility or its regulation (44). The cdG synthase DmxB, which is only expressed during starvation, stimulates EPS production during development (45). These observations established the involvement of cdG in T4P-mediated motility and possibly biofilm formation in M. xanthus.

A new cdG binding domain, known as MshE_N, was discovered in the N-terminus of MshE, a PilB orthologue for the mannose sensitive hemagglutinin (Msh) pilus in V. cholerae (46). The signature of the MshE_N domain consists of a tandem repeats of a cdG-binding motif with the consensus sequence of $RLG(x^2)LV(x^2)GLI(x^4)L(x^3)L(x^2)Q$ (where x could be any residue) (47). These motifs are conserved in the N-terminus of PilB (PilB_N) or its equivalent PilF in many bacteria including M. xanthus, Chloracidobacterium thermophilum, and Thermus thermophilus (48). Studies with C. thermophilum PilB in vitro demonstrated that it binds cdG with its PilB_N domain while its C-terminal ATPase domain bind ATP and ADP. Interestingly, the bindings of cdG and ADP to C. thermophilum PilB mutually affected the binding of the other (48), indicating reciprocal communications

between its N- and C-terminal domains. These results suggest that cdG may bind to *M. xanthus* PilB and possibly bifurcate its dual functions in motility and biofilm regulation.

Here, *M. xanthus* PilB is shown to be a genuine cdG effector by differential scanning fluorimetry (DSF), and we performed a systematic genetic analysis to probe the regulation of PilB by cdG in *M. xanthus*. Mutations in PilB_N were constructed such that its cdG binding signature either more closely match with or diverged from the consensus sequence. Our results suggest that the binding of cdG may serve as a switch to bifurcate the outputs from *M. xanthus* PilB to regulate its functions in motility and biofilm formation.

RESULTS

M. xanthus PilB is a bona fide cdG effector protein

To determine if M. xanthus PilB is a genuine cdG effector protein, its PilB $_{\rm N}$ domain (the first 139 amino acids) with a C-terminal histidine tag was expressed in E. coli and purified for analysis by DSF (49). The intrinsic thermal stability of the protein was first analyzed in the absence of cdG. As shown in Fig. 1A, the thermogram of PilB $_{\rm N}$ showed a monophasic unfolding profile as expected for a single domain protein. The analysis of the melting curve (Fig. 1B) indicated that M. xanthus PilB $_{\rm N}$ has a transition midpoint (T_m) at 54.7°C, which will be referred as the intrinsic melting temperature or the melting temperature in the absence of cdG (T_m). The thermostability of PilB $_{\rm N}$ was next examined in the presence of cdG to examine if it could bind to cdG. As shown in Fig. 1, the protein displayed a similar monophasic unfolding curve in the presence of cdG. Its melting temperature in the presence of cdG (T_m) increased to 59.0°C, indicating a cdG-induced temperature shift (ΔT_m) of 4.3°C (Fig. 1). The increase in thermostability indicates that M. xanthus PilB indeed binds cdG and is a bona fide cdG effector protein as has been suspected.

Site-specific mutagenesis of the MshE_N domain of M. xanthus PilB

The biological significance of cdG-binding to *M. xanthus* PilB was probed by a systematic mutational analysis. A total of 15 mutations targeting the conserved MshE_N domain of

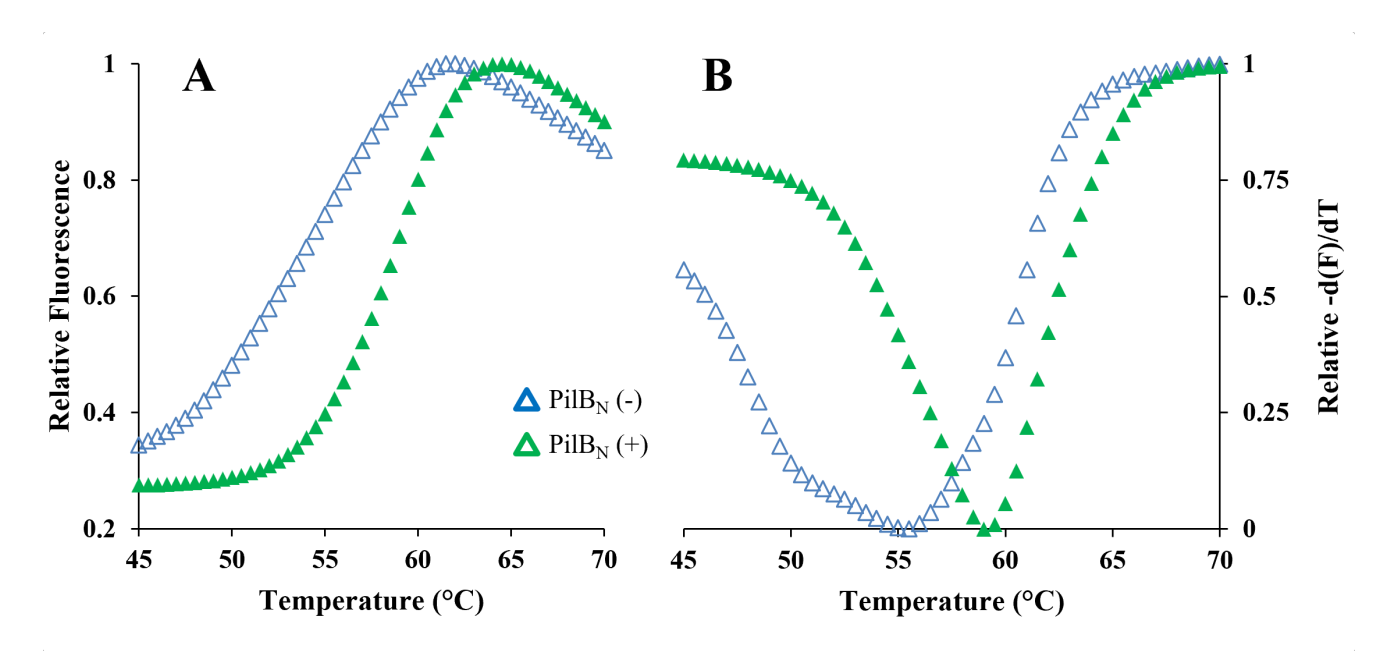


FIG 1 *M. xanthus* PilB is a cdG effector protein. Ten micromolars of PilB $_{\rm N}$ in the absence (–) and presence (+) of 750 μ M cdG was monitored for thermostability using DSF. The relative fluorescence of the thermogram (A) and its first derivative for the determination of T_m (B) are shown. In panel A, the maximum fluorescence signal is normalized to 1. In panel B, the lowest point of each curve was set to zero (0), and the maximum, to 1. The averages from three independent experiments, each performed in triplicate, are shown. See text for details.

M. xanthus PilB were generated to potentially alter its cdG binding affinity and protein conformations (Fig. 2). Here, two general categories of mutants were constructed (Fig. 2B and C). The first category aimed to mutagenize the conserved resides in M. xanthus PilB to other amino acids; similar substitutions in V. cholerae MshE_N are known to reduce cdG binding with clear biological consequence on motility, biofilm, and piliation for selected mutations in V. cholerae (47). The second category targeted existing residues in M. xanthus PilB that differed from the conservation in MshE_N domains. These residues were identified by sequence comparisons, and they were then mutagenized to the more conserved amino acids; no equivalent substitutions of this type have been made or studied in MshE or other PilB orthologues.

The first category includes the substitution of two conserved glycine (G) with leucine (L) and four conserved L or isoleucine (I) with alanine (A), either individually or in combination (Fig. 2). These substitutions were chosen based on similar mutations in MshE and the phenotypes of the resulting *mshE* mutants related to the *V. cholerae* the MshA T4P (47). More specifically, the residues targeted here were L5 and G6 in the first repeat and I34, G35, L49, and L53 in the second (Fig. 2). These residues were

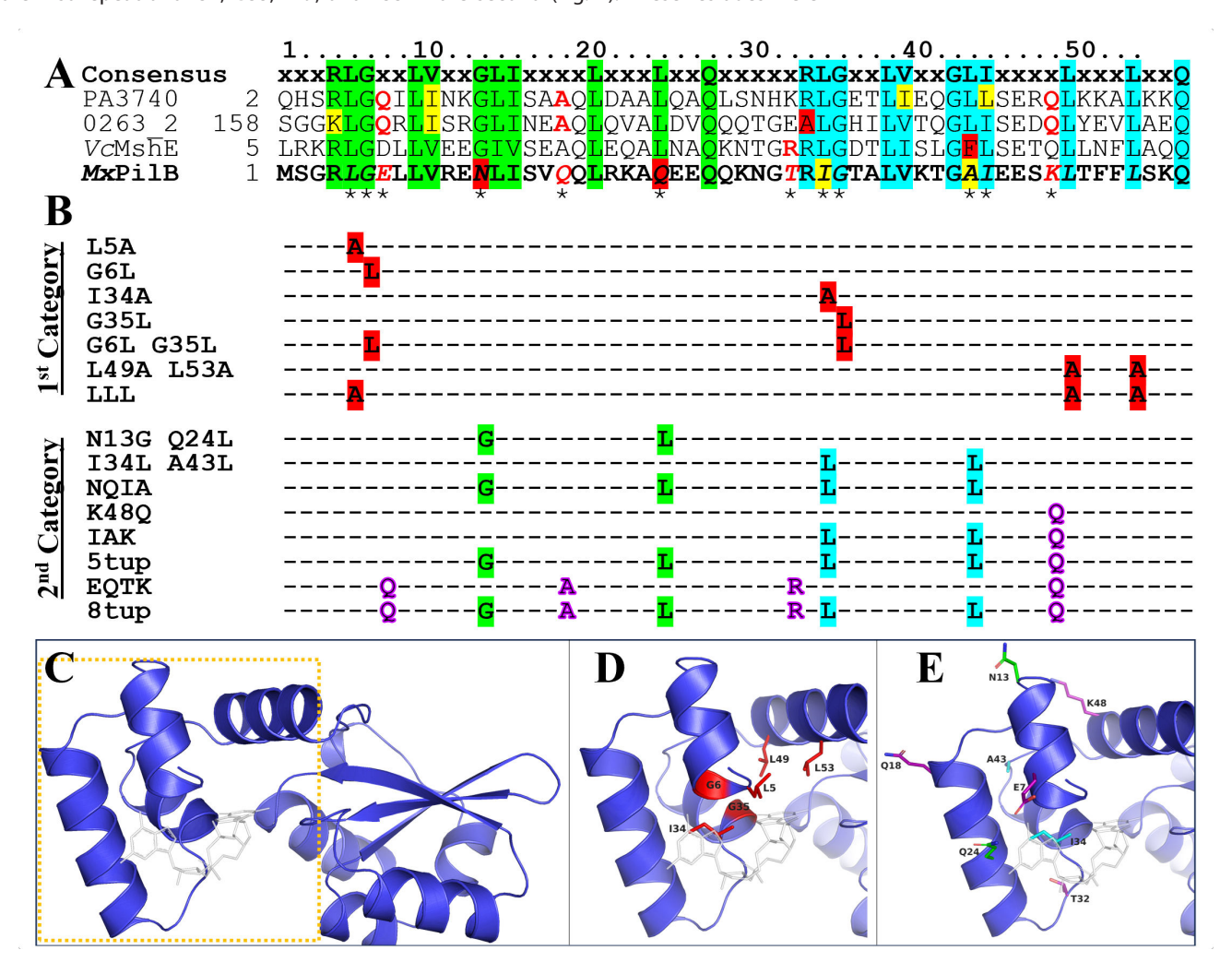


FIG 2 Alignment and summary of *pilB* mutations. (A) In the sequence alignment, the two conserved motifs are highlighted in green (Motif I) and aqua (Motif II), respectively. The MshE_N domains of *V. cholerae* (*Vc*) *MshE*, *M. xanthus* (*Mx*) PilB, Paer_PA3740, and Dgeo_0263_2 are shown. The residues in these domains that are identical to the consensus are highlighted as in the two conserved motifs. The conserved and unconserved changes are highlighted in yellow and red, respectively. Asterisks (*) indicate *Mx*PilB residues, also in bold and italics, that were mutagenized in this study. (B) The two categories of mutations are listed with the resulting substitutions indicated. (C) The structural model of PilB_N with a bound cdG (gray). The boxed region in dashed line is shown in D (first category) and E (second category) wherein the residues targeted for mutagenesis are shown with side chains colored as in B except G6 and G35 whose backbones are colored in red.

Downloaded from https://journals.asm.org/journal/jb on 11 September 2023 by 2001:468:c80:610b:b9c3:185c:cd77:cce1

mutagenized to construct four single (L5A, G6L, I34A, and G35L), two double (G6L G35L and L49A L53A), and one triple (L5A L49A L53A or LLL) substitution mutations (Fig. 2). These mutations all targeted residues on the ligand binding side of PilB_N as shown in by structural modeling of PilB_N generated by Alphafold (50) (Fig. 2C and D). To reiterate, the equivalent MshE_N variants of these seven mutations in the first category were found to have significantly reduced affinity for cdG with clearly observable biological consequences (47).

The second category has mutations that made M. xanthus PilB more similar with the MshE_N consensus motifs (Fig. 2). M. xanthus PilB differs from the two conserved cdG-binding motifs at four positions (Fig. 2A). These are residues Asparagine 13 (N13) and Glutamine 24 (Q24) in the first motif and I34 and A43 in the second (Fig. 2A and E); they correspond to G, L, L, and L in the consensus sequence, respectively. Three mutations were constructed to target these residues, and they are the N13G Q24L I34L A43L (NQIA) quadruple as well as the N13G Q24L and the I34L A43L double substitutions (Fig. 2B). It is noted Q24 and I34 are predicted to be in contact with a bound cdG, but not N13 and A34 (Fig. 2E). The latter two are on the opposite side of the cdG binding pocket, and they are predicted to be in loops between the first and the second helices and between the third and fourth helices, respectively (Fig. 2E). There are five additional mutations in this category that targeted Glutamate 7 (E7), Q18, Threonine 32 (T32), and Lysine 48 (K48). Three of these residues, E7, Q18, and K48, were targeted based on alignments with PA3740 and Dgeo_0263_2 (Fig. 2A) because they had the highest affinity for cdG among MshE_N domains experimentally examined (47). Modeling indicates that E7 is near or in the cdG binding pocket, while Q18 or K48 are exposed on the other side of the modeled PilB_N structure away from the bound ligand (Fig. 2E). T32 was chosen because it most frequently aligns with a positively charged arginine (R) or lysine in MshE_N domains in multisequence alignments (47) (data not shown). Modeling indicates that this residue has the potential to interact with a bound cdG (Fig. 2E). Mutations here include the K48Q single, the I34L A43L K48Q (IAK) triple and the E7Q Q18A T32R K48Q (EQTK) quadruple substitution mutations. K48Q and EQTK were each combined with the NQIA mutation above to produce a quintuple (5tup) and an octuple (8tup) substitution. The eight mutations in this category (Fig. 2B) were constructed for the possible enhancement of cdG binding and alteration of protein conformation.

In summary, a total of 15 mutations were constructed with seven in the first and eight in the second category, respectively (Fig. 2). All of these mutations were generated with the full-length wild-type pilB (pilB⁺) gene as the template on a plasmid that integrates on the M. xanthus chromosome at a phage attachment site (51) (Table S1). Details on the construction of these mutations are described in the Materials and Methods (Table S2) and all mutations were confirmed by DNA sequencing prior to their biological characterization.

M. xanthus pilB mutants displayed a spectrum of S-motility phenotypes

Plasmids with the above mutations and the $pilB^+$ allele were transformed into an M. xanthus pilB deletion (ΔpilB) mutant for complementation (Table S1). The T4P-dependent S motility of the resultant M. xanthus strains was first analyzed on soft agar plates (0.4% agar) (Fig. S1). Shown in Fig. 3 are the results from three independent experiments, each performed with four or more replicates. Among the seven mutants in the first category, G35L was like the wild type, while the G6L mutant showed a small but statistically significant increase (S⁺⁺) in S motility over the wild type. These two mutations are the equivalents in the two repeated motifs (Fig. 2), and their different phenotypes suggest possible differentiation in function for the two repeats. Among the eight mutants in the second category, K48Q was comparable with the wild type, and two mutants, NQIA quadruple and N13G A43L double, showed increased S motility. All the other mutants, regardless of their categories, showed various degrees of decreased S motility relative to the wild type. These S-motility phenotypes of the mutants were confirmed by a second motility assay on hard agar surfaces (Fig. S2 and S3), which allow both the

T4P-dependent S motility and the T4P-independent A motility to function (52). Since pilB deletions have no effect on A motility (33), the net differences among strains in this assay reflect difference in S motility attributable to the different pilB mutant alleles. The results on hard agar (Fig. S3) are consistent with those on soft agar, demonstrating consistent S motility phenotypes for all mutants.

In summary, of the 15 pilB mutants with genetic alterations in the PilB_N cdG-binding domain, two resembled the wild type (S⁺), three displayed increased S motility (S⁺⁺), and the rest exhibiting a reduction in S motility relative to the wild type (referred to as S⁻ in later discussions for convenience) (Fig. 3; Fig. S3). There is no strict correlation between the S-motility phenotype with the designated category of a given mutant.

Eight mutants produced PilB at the wild-type level

PilB protein levels were examined by immunoblotting to facilitate the interpretation of phenotypes of the pilB mutants. Fig. 4 presents the averages from three independent biological experiments each conducted in quadruplicate samples (Fig. S4). Of the 15 mutants, eight showed wild-type levels of PilB, while the remaining seven had lower levels in comparison. Of the seven mutants with lower PilB levels, all except G6L are associated with the S⁻ phenotype (Fig. 4); this was expected because S motility depends on T4P, which requires PilB for assembly. The G6L mutant is an exception in that its PilB level is clearly lower than that of the wild type, yet it has an S⁺⁺ phenotype (Fig. 3 and 4). The eight mutants with wild-type PilB levels include six of the eight mutants in the second category and two of the seven in the first, suggesting that PilB variants

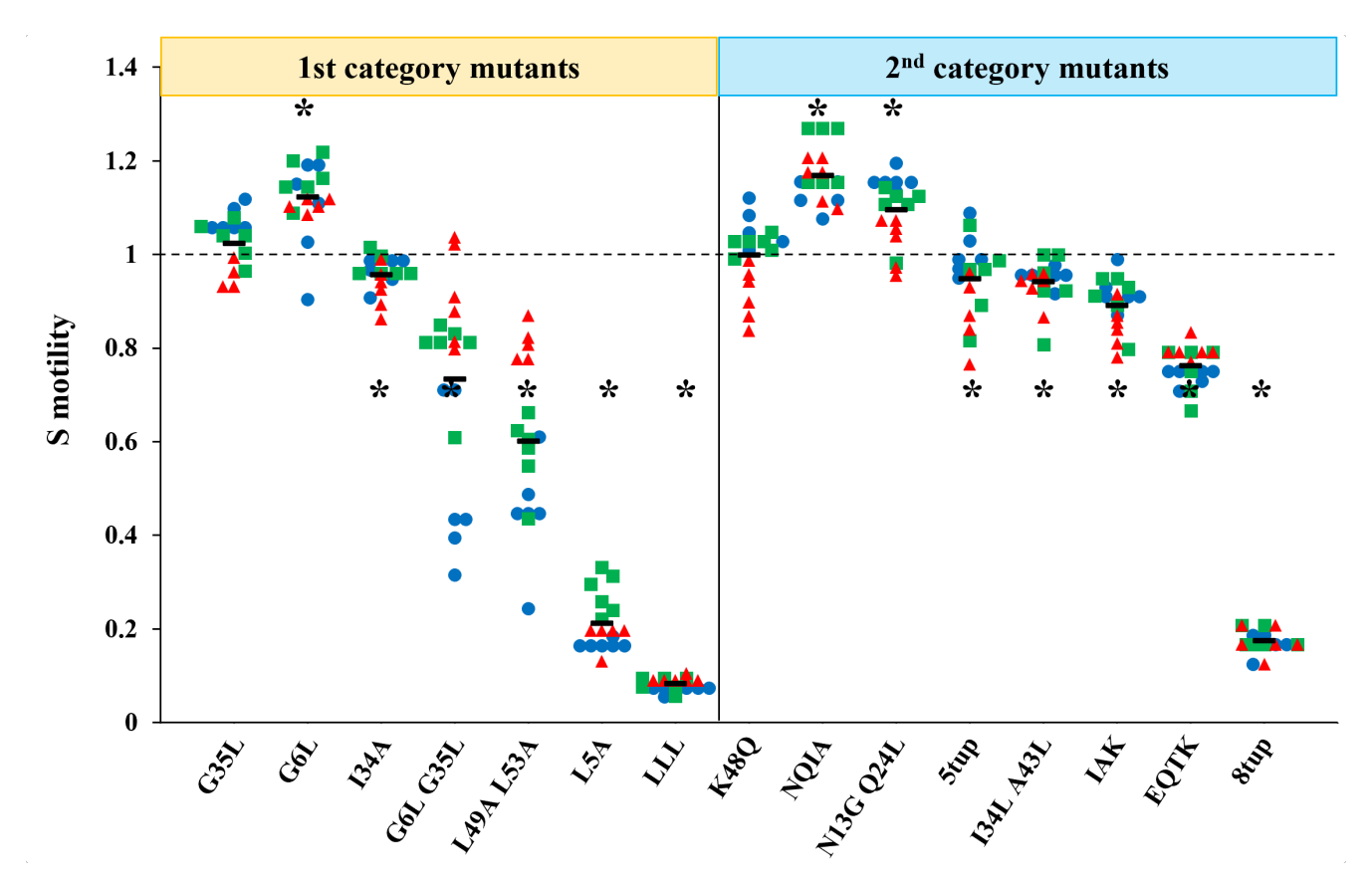


FIG 3 Mutations in the MshE_N domain of PilB affect S motility. The colony expansion for each mutant on soft agar plates relative to the wild type is shown. The data were from three independent experiments with the replicates from each represented by the same color and shape. The black bar indicates the average from the entire data sets. The size of each mutant colony was analyzed relative only to those of the wild-type (YZ3621) and the pilB mutant (YZ3625) controls on the same plate to minimize the impact of plate variations. Asterisk (*) signifies that a mutant is statistically different from the wild type from the aggregates of all measurements with a P values < 0.05 as determined by Student's t-test.

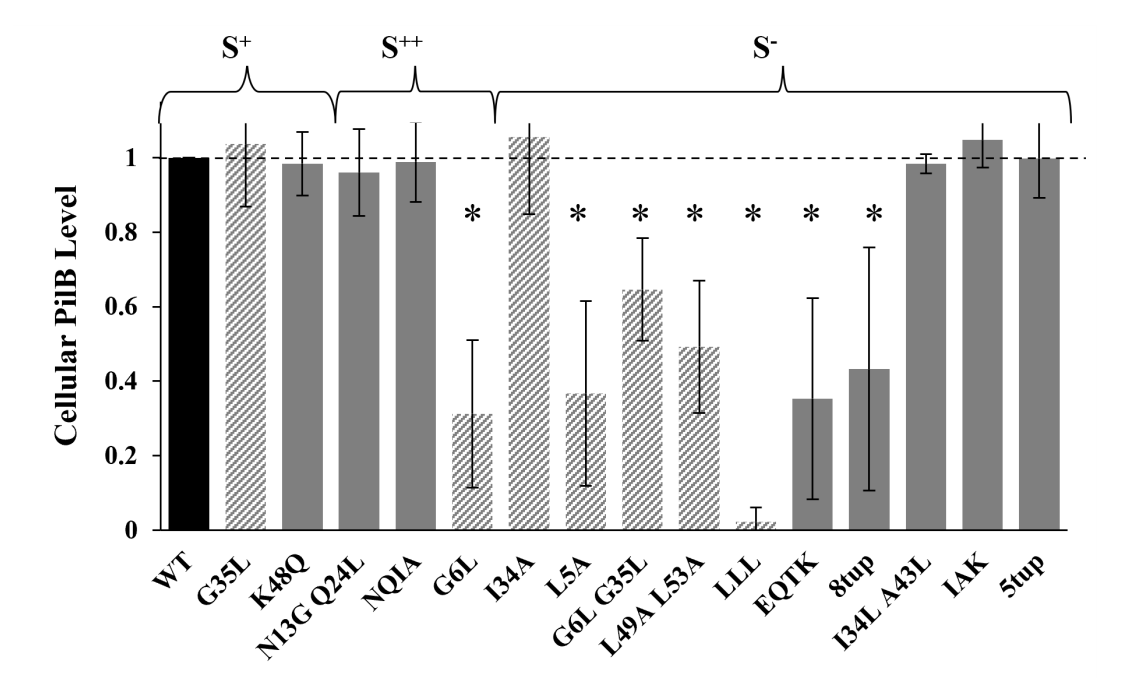


FIG 4 Cellular PilB protein levels. The quantification of the protein level of each PilB variant normalized to the wild type by immunoblotting is shown. The values are the averages from three independent biological experiments. Asterisks (*) denote protein levels statistically different from the wild type (P < 0.05). Mutants in the first and second categories are shown in dashed and solid gray, respectively, with the wild type in black. A representative immunoblot is shown in Fig. S4.

closely matching the consensus have a higher tendency to be stable *in vivo*. Among these mutants (Fig. 3), two are like the wild type (S^+), two showed the S^{++} phenotype, and the other four had varying degrees of S motility defects (S^-). Of the two in the first category, one is S^+ , and the other is S^- . Of the six in the second, one is S^+ , two are S^{++} , and the remaining three are S^- . These eight mutants with wild-type levels of PilB were selected for further analysis in this remainder of this study.

Piliation levels are influenced by six of the eight PilB_N mutations

M. xanthus S motility as analyzed on agar plates (Fig. 3; Fig. S1-S3) requires both T4P and EPS to function (30). EPS, which is proposed to be the trigger for T4P retraction (53), is known to affect piliation levels in M. xanthus (30). The capacity of the eight selected PilB variants to function as the T4P assembly ATPase was analyzed by piliation levels in an EPS⁻ background with the difE gene deleted (30, 54). In this experiment, wild-type and mutant alleles of pilB were transformed into YZ3640 (ΔpilB ΔdifE) (Table S1), and the resulting strains were assessed for their pilin pools and piliation levels as previously described (55, 56) (Fig. 5A; Fig. S5 and S6). The four mutants with decreased S motility (I34A, I34L A43L, IAK, and 5tup) all had statistically reduced piliation levels relative to the wild type (Fig. 5A). This was largely expected because S motility correlates with PilA expression and piliation levels (57). These results imply that cdG binding can regulate the T4P assembly activity of PilB as a means to affect T4P-dependent motility in M. xanthus. At the molecular levels, the binding of cdG to the N-terminus of PilB is inferred to allosterically regulate the activity of the ATPase domain at the C terminus of this protein. These results are consistent with observations with MshE mutant variants in V. cholerae (47) and the communications between the N- and the C-termini of C. thermophilum PilB (48).

The correlation above between piliation and S motility was only observed in the S⁻ pilB mutants, and it does not extend to the S⁺ and S⁺⁺ ones (Fig. 3; Table S3). The two mutants with wild-type S motility (S $^+$) (G35L and K48Q) exhibited approximately 50% higher piliation levels compared to the wild type, despite their similar levels of S motility

Month XXXX Volume 0 Issue 0

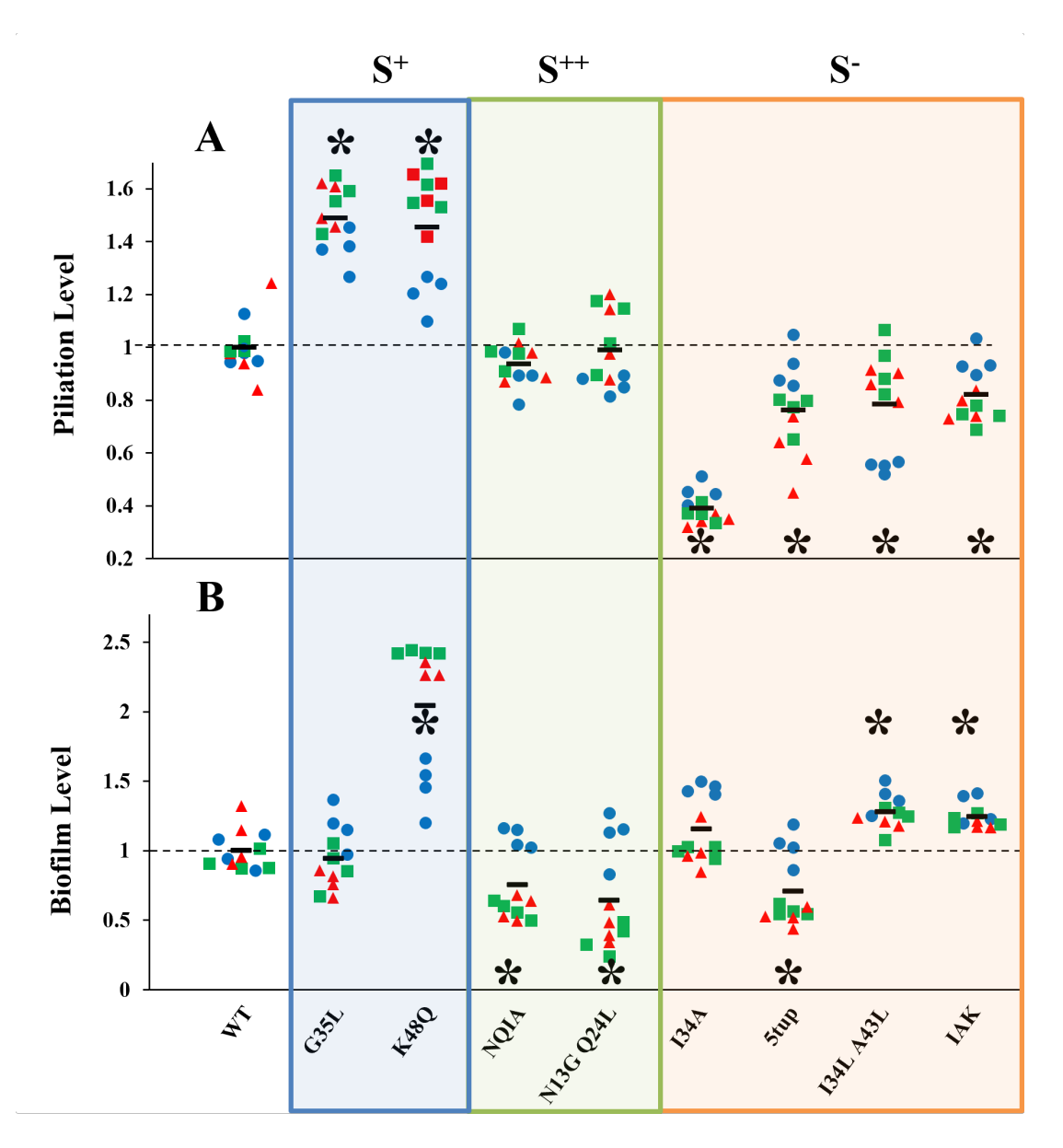


FIG 5 PilB mutants influence levels of piliation and biofilm independently of each other. Levels of piliation (A) and biofilms (B) of mutants relative to the wild type are shown. Results are from three independent biological replicates, with data points from the same experiment represented by a distinctly colored shape. The values of the wild type are normalized to one as represented by the horizontal dashed line. The mutants are grouped by their S motility phenotypes. Asterisks (*) indicate statistical differences from the wild type with P < 0.05. Piliation levels (A) were analyzed by measuring the amounts of pilins in a physically shearable pilus fraction (see Fig. S5) (55). Biofilm levels (B) were from the quantification of submerged biofilms in 96-well plates after 24 h of incubation (39).

(Fig. 5A). Likewise, the two mutants with the S⁺⁺ phenotype (N13G Q24L and NQIA) both displayed piliation levels comparable to the wild type, despite their increased S motility. These findings indicate that PilB can impact S motility either independently of or in addition to its T4P assembly activity. These conclusions are further supported by the observations with the S⁻ mutant group. For instance, the I34A mutant showed the most significant decrease in piliation level, with a reduction of ~60% (Fig. 5A). However, the extent of its reduction in S-motility is like those of the 5tup, the I34L A43L and the IAK mutants (Fig. 3), all of which clearly exhibit higher levels of piliation than I34A (Fig. 5A). In other words, the combined results on piliation (Fig. 5A) and S motility (Fig. 3) imply that the genetic alteration of cdG binding by PilB can influence factors other than piliation,

which are also relevant to S motility as evaluated by colony expansion on agar plates (Fig. 3; Fig. S1).

Mutations in PilB_N domain can alter EPS and biofilm levels independently of **T4P** assembly

As has been alluded to earlier, EPS is another key player in M. xanthus S motility besides T4P (30, 58, 59). Here, we analyzed the levels of submerged biofilms to quantify M. xanthus EPS levels as previously described (39) (Fig. 5B; Table S3). The phenotypes of only two out of the eight mutants examined, K48Q and 5tup, could be explained by the positive regulation of EPS/biofilm by piliation as previously reported (30, 34, 36, 40). The hyperpiliated K48Q mutant overproduced EPS, while the hypopiliated 5tup mutant underproduced. In contrast, the other six mutants displayed non-correlating or opposite phenotypes in piliation and EPS levels. The G35L mutant, while hyperpiliated, produced wild-type levels of EPS. The two mutants, NQIA & N13G Q24L, underproduced EPS (Fig. 5B) while exhibiting wild-type levels of piliation (Fig. 5A). Of the remaining three mutants with reduced piliation levels, the I34A mutant has the wild-type EPS phenotype, while the I34L A43L and the IAK overproduced EPS.

It was shown previously that the EPS-signaling and T4P-assembly activities of PilB could be genetically separated (40). The observations here provide evidence that the binding of cdG to PilB can modulate the activity of PilB in signaling EPS production as an independent output from its T4P assembly activity. In other words, cdG may interact with M. xanthus PilB to bifurcate its dual functions in regulating motility and biofilm formation as a universal second messenger of bacterial lifestyles.

DISCUSSION

The regulation of motility and biofilm formation by cdG has been extensively investigated in flagellated bacteria (10, 12, 13). In contrast, little is known on how this regulation occurs in motile bacteria without any flagellum. T4P-powered bacterial surface locomotion is arguably the best known and most extensively studied among the non-flagellated motility systems (29). Here, we used M. xanthus as the model to investigate how M. xanthus PilB and its interactions with cdG may regulate motility and biofilm formation in this bacterium with T4P-mediated motility. We confirmed that M. xanthus PilB is a genuine cdG effector using a heterologously expressed protein (Fig. 1). Genetic analysis showed that all mutations in M. xanthus PilBN domain led to distinctive phenotypes different from the wild type. These findings provide insights into how PilB may interact with cdG to regulate the motile and the biofilm state in a model bacterium with T4P-powered motility and without any flagellum.

There have been investigations on the interactions of cdG with the T4P assembly ATPase in the T4P systems in V. cholerae and C. perfringens. It was the study of the MshE assembly ATPase in the V. cholerae MshA pilus system that led to the discovery of the MshE_N cdG binding domain (46, 47) that is also present in the N terminus of C. perfringens PilB (60). The picture that emerged from V. cholerae and C. perfringens is that cdG binds to the N terminus of MshE or PilB likely to stimulate T4P assembly (47, 60, 61). It should be noted that neither the MshA pilus nor the C. perfringens T4P serves as a motility apparatus. It was thought initially that the C. perfringens T4P system was involved bacterial motility, but later investigations clarified that the colony spreading of "hypermotile" C. perfringens mutants was due to the formation of cellular filaments related to cell division instead of T4P (62). C. perfringens is a non-flagellated anaerobe, and the biological role of its T4P remains to be established. V. cholerae is motile by flagellated swimming motility with no T4P-mediated motility (18). Its MshA pilus promotes biofilm formation as an adhesin and an inhibitor of swimming motility by tethering cells to solid surfaces (47). The stimulation of V. cholerae MshA pilus assembly by cdG in the broader sense is in line with the established paradigm of motility and biofilm regulation in flagellated bacteria, that is, the increase in cdG signaling leads to increased MshA pilus production to promote biofilm formation and inhibit flagellated

Downloaded from https://journals.asm.org/journal/jb on 11 September 2023 by 2001:468:c80:610b:b9c3:185c:cd77:cce1

motility (47). Because the T4P is not used as a motility apparatus in *V. cholerae*, it is an open question whether the model of MshE regulation by cdG would be applicable to *M. xanthus* PilB which does assemble a pilus as a motility apparatus (63).

Indeed, observations here suggest that there are likely differences between the regulation of the M. xanthus PilB and V. cholerae MshE by cdG. For instance, there are clear phenotypic differences between V. cholerae and M. xanthus strains with equivalent mutations in their T4P assembly ATPases MshE and PilB. The MshE mutant variants with L54A L58A double or L10A L54A L58A triple substitutions were found to be active in pilus assembly despite their lack of or significant reduction in cdG binding (47). As such, they were suggested to be constitutively active in T4P assembly without requiring cdG stimulation. The two M. xanthus PilB equivalents are L49A L53A and LLL (Fig. 2), and both mutants are significantly reduced in T4P-mediated motility (Fig. 3). The piliation of these mutants was not examined because of their significantly diminished PilB levels (Fig. 4), but it is likely that their S⁻ phenotypes are due to a lack or reduction of piliation. In contrast, their equivalent MshE proteins are likely produced at near or above wild-type levels because their V. cholerae mutants were found to be hyperpiliated, which requires the functioning of MshE. Another example is the M. xanthus G6L mutant. This mutant, which exhibits significantly reduced PilB levels (Fig. 4), has a surprising S⁺⁺ phenotype (Fig. 3). It can, therefore, be inferred to be piliated above a certain threshold (57). In contrast, the V. cholerae equivalent, the G11L mutant, showed enhanced swimming motility with no detectable piliation (47). These contrasting observations suggest that despite the conservations of the orthologous T4P systems and their components at the structural and organizational levels, their biological function likely has an oversized influence on the regulation and functioning of these systems in different biological context. In other words, whether a T4P system functions as a motility apparatus or not may dictate how it is regulated by cdG as the master regulator of biofilm and motile states in bacteria.

A more complex model beyond a simplistic allosteric regulation of ATPase activity appears necessary to explain the observations with mutations in the two conserved tandem motifs of PilB and its orthologues (Fig. 2). This is because there are indications that the two repeats may have distinctive functions biologically, besides contributing to specific ligand-protein interactions at the structural level. The two motifs in MshE_N were shown to essentially have symmetrical or identical interactions with the twin GMPs in cyclic di-GMP by X-ray crystallography (47). In V. cholerae MshE, the L25 and L29 pair in the first motif is equivalent to the L54 and L58 pair in the second (Fig. 2). MshE_N proteins with one or the other of these two pairs mutated led to similar decreases in cdG binding affinity (47). However, an mshE mutant with the L54A L58A substitution, but not L25A and L29A, was reported to be hyperpiliated (47). In M. xanthus, among the pilB mutants in the second category (Fig. 2), those with mutations in the first cdG-binding motif (N13G Q24L, NQIA and 5tup) tend to show decreased EPS levels with varying consequences on piliation (Fig. 5). In comparison, those with mutation only in the second cdG-binding motif (K48Q, I34L A43L and IAK) are observed to have elevated EPS levels with varying degrees of effect on piliation (Fig. 5). These observations argue that a simplistic allosteric effect of cdG on the ATPase activity of PilB and its orthologous is insufficient to explain the functional consequences of cdG binding. It could be speculated that cdG binding to PilB may impact interactions of PilB with other proteins unrelated to T4P assembly. It is necessary to conduct further investigations to fully appreciate the functions of the PilB-cdG interactions in bacteria that use T4P to facilitate motility and biofilm formation.

MATERIALS AND METHODS

Strains and growth conditions

Strains and plasmids used in this study are listed in Table S1. *M. xanthus* was grown and maintained at 32°C on Casitone-yeast extract (CYE) agar or in CYE liquid medium

(64). *E. coli* strain XL1-Blue (Stratagene) was used for plasmid construction and BL21 (DE3) (Novagen) for heterologous expression of $PilB_N$ variants. They were grown and maintained at 37°C on Luria-Bertani (LB) agar or in LB broth (Fisher). Unless otherwise stated, all plates contained 1.5% agar. When appropriate, kanamycin or ampicillin was added to media at a final concentration of 100 μ g/mL.

Plasmid and strain construction

Sixteen plasmids (Table S1) with the wild-type and mutant alleles of full length pilB were created using pKY101 (65) as the expression vector in M. xanthus. pKY101 is integrative in M. xanthus with the Mx8 phage attachment site (att) (64). These plasmids may be divided into three groups based on how they were constructed. The first group of three plasmids includes pWAS100 (wild type), pWAS101 (G6L), and pWAS102 (L5A). They were constructed by PCR with pWB571 as the template (40) using Phusion DNA polymerase (New England Biolabs) with primers (Table S2) designed to introduce the desired mutations. PCR fragments were digested with Ndel and Xbal and inserted into the same sites in pKY101. The second group of 11 plasmids was constructed by site directed mutagenesis using the Q5 High Fidelity DNA polymerase mutagenesis kit (New England Biolabs) and different starting plasmids as below. pWAS100 was the template for pUA102 (N13G Q24L), pUA103 (I34L A43L), pUA105 (I34A), pUA106 (G35L), pUA108 (L49A L53A), and pUA110 (K48Q). pWAS101 was the template for pUA107 (G6L G35L); pWAS102, for pUA109 (LLL); pUA102, for pUA104 (NQIA); pUA103, for pUA111 (I34L A43L K48Q); and pUA104, for pUA112 (5tup). The third group of two plasmids, pUA113 (EQTK) and pUA114 (8tup), contained customer synthesized fragments in pUC57 (Eurofins Scientific). These fragments and pUA110 were digested with Ndel and KpnI and ligated. These plasmids were electroporated (7) into DK10416 (ΔpilB) (51) and YZ3640 (ΔpilB ΔdifE) (Table S1) for the examination of complementation and piliation levels (53), respectively. YZ3640 was constructed from DK10416 (ΔpilB) by the deletion of difE using pWB118, which contains an in-frame $\triangle difE$ deletion, as previously described (35).

Ten plasmids for the expression of the $PilB_N$ variants with a C-terminal 6× histidine tag were constructed (Table S1) using pET-15b (Novagen) as the vector. The first 417 base pairs of a mutated pilB gene from an appropriate plasmid above were PCR amplified (Table S2), digested by Ndel and Xhol and ligated into the same sites of pET-15b.

All plasmids constructed in this study were confirmed by DNA sequencing at the Virginia Tech Genomics Sequencing Center.

Purification of PilB_N variants and DSF analysis

The expression of $PilB_N$ variants in BL21 (DE3) was induced by 0.5 mM isopropylthio- β -galactoside for 16 h at 20°C with shaking at 250 rpm. All 10 proteins were purified by fast protein liquid chromatography (FPLC) using Ni-NTA and SEC columns as was previously described (66) with the omission of heat treatment. The activity buffer (50 mM of TAPS N-[Tris(hydroxymethyl)methyl]–3-aminopropanesulfonic acid) and Tris each at pH 8.7, 75 mM KCl, 50 mM NaOAc, and 5 mM MgCl₂) with 5% glycerol was used as the gel filtration buffer.

DSF experiments were carried out using a C1000 thermocycler (BioRad) coupled to a CFX96 Real-Time (BioRad) PCR detection system. PilB $_{\rm N}$ variants at 10 μ M in activity buffer with 50 μ M ZnCl $_{\rm 2}$ and 5× SYPRO Orange dye (Thermo Fisher) were analyzed in the absence or presence of 750 μ M cdG (InvivoGen). Fluorescence was monitored from 20 to 90°C in 0.5°C increments with 30-s intervals. Derivatization of the melt curve was used to determine the melting temperature (T_m) of a sample by the first derivative curve method (67). Each sample was analyzed in three separate experiments in triplicate with the average of the results presented in the manuscript.

Determination of PilB protein levels

The level of PilB protein in M. xanthus strains was examined by immunoblotting with anti-M. xanthus PilB antibodies (63) with whole cell lysates from 1×10^7 cells loaded for SDS-PAGE and subsequent analysis. Goat anti-rabbit antibodies conjugated to horseradish peroxidase (Thermo Fisher) were used as the secondary antibodies at a 1:15,000 dilution. Blots were developed using SuperSignal West Pico PLUS chemiluminescent substrate (Thermo Fisher). The chemiluminescence signal was captured with a 1.5-s exposure using a ChemiDoc MP imaging system (Bio-Rad). For quantification, the pixel densities of the samples were analyzed using ImageJ (68). Data presented in the manuscripts are from three separate experiments with each conducted with triplicate samples.

Phenotypic analysis

To examine the S motility of the mutants, cells in log phase of growth in CYE were harvested and resuspended to an optical density at 600 nm (OD₆₀₀) of 5 in MOPS buffer (10 mM morpholinepropanesulfonic acid [pH 7.6], 10 mM MgSO₄, and 10% [vol/vol] India ink). Five microliters of the cell suspension from four different strains was spotted onto either a soft (0.4% agar) or a hard (1.5% agar) CYE plate. These four strains include two mutants to be examined, as well as YZ3621 ($\Delta pilB$ att::pilB) as the wild-type control and YZ3625 ($\Delta pilB$) (Table S1) as the pilB mutant control. After incubation for 5 d at 32°C, the diameters of the colonies were measured. Colony expansion was calculated by subtracting the initial diameter of the spotted colony marked by India ink. The diameter of the $\Delta pilB$ mutant on the hard agar plates was also subtracted in data processing to eliminate the impact of A motility on colony expansion. In total, 18 colonies from three separate experiments were measured for each strain on each plate type. S motility of each mutant was normalized to that of the YZ3621 wild-type control to minimize plate variations.

M. xanthus submerged biofilms were analyzed using 96-well plates as previously described (39) with the crystal violet absorbance measured at 590 nm instead of 600 nm. The analysis of piliation levels was conducted as previously described (53) using antibodies against *M. xanthus* PilA (57). The results presented in this manuscript are averages from three independent experiments, each conducted with multiple replicates.

PilB_N structural modeling

The structural model of $PilB_N$ was generated using AlphaFold (50). cdG was modeled into the $PilB_N$ structure as in $MshE_N$ (47) using DALI (69). The presentation of the structure and labeling were performed using PyMOL (70).

ACKNOWLEDGMENTS

This work was partially supported by the National Science Foundation grants MCB-1417726 and MCB-1919455 to Z.Y. The Yang laboratory received pilot grants from the Lay Nam Chang Dean's Discovery Fund and the Center for Emerging, Zoonotic and Arthropod-borne Pathogens. U.A. was supported by the Virginia Tech PREP program. K.J.D. was the recipient of a GSDA and the Lewis Edward Goyette Fellowships as well as the Liberati Scholarship from Virginia Tech.

K.J.D., and Z.Y. designed research, analyzed data, and wrote the manuscript. K.J.D. performed experiments. S.S. performed structural modeling. U.A., and W.S. constructed plasmids and mutations. Kristine Yarnoff, a Fralin SURF fellowship recipient, assisted in this study.

A special gratitude to Dr. Dan Wall for the early alert of the work on MshE_N . We thank Tori Shimozono and Jay Ramos for critical reading of this manuscript and Dr. Florian Schubot for helping with structural modeling.

There is no conflict of interest to declare.

AUTHOR AFFILIATION

¹Department of Biological Sciences, Virginia Tech, Blacksburg, Virginia, USA

PRESENT ADDRESS

Keane J. Dye, Department of Microbiology and Immunology, Uniformed Services University of the Health Sciences, Bethesda, Maryland, USA

AUTHOR ORCIDs

Zhaomin Yang http://orcid.org/0000-0002-2044-6793

FUNDING

Funder	Grant(s)	Author(s)
National Science Foundation (NSF)	MCB-1417726, MCB-1919455	Zhaomin Yang

AUTHOR CONTRIBUTIONS

Keane J. Dye, Conceptualization, Data curation, Formal analysis, Investigation, Methodology, Project administration, Validation, Visualization, Writing – original draft, Writing – review and editing | Safoura Salar, Formal analysis, Methodology, Visualization | Uvina Allen, Data curation, Investigation, Methodology | Wraylyn Smith, Data curation, Investigation, Methodology | Zhaomin Yang, Conceptualization, Formal analysis, Funding acquisition, Investigation, Methodology, Project administration, Resources, Supervision, Visualization, Writing – review and editing

ADDITIONAL FILES

The following material is available online.

Supplemental Material

Supplemental figures and tables (JB00221-23-s0001.pdf). Fig. S1 to S6 and Tables S1 to S3.

REFERENCES

- Locke JCW. 2013. Systems biology: how bacteria choose a lifestyle. Nature 503:476–477. https://doi.org/10.1038/nature12837
- Oggioni MR, Trappetti C, Kadioglu A, Cassone M, Iannelli F, Ricci S, Andrew PW, Pozzi G. 2006. Switch from planktonic to sessile life: a major event in pneumococcal pathogenesis. Mol Microbiol 61:1196–1210. https://doi.org/10.1111/j.1365-2958.2006.05310.x
- 3. Nakamura S, Minamino T. 2019. Flagella-driven motility of bacteria. Biomolecules 9:279. https://doi.org/10.3390/biom9070279
- Moens S, Vanderleyden J. 1996. Functions of bacterial flagella. Crit Rev Microbiol 22:67–100. https://doi.org/10.3109/10408419609106456
- Belas R. 2014. Biofilms, flagella, and mechanosensing of surfaces by bacteria. Trends Microbiol 22:517–527. https://doi.org/10.1016/j.tim. 2014.05.002
- Rossez Y, Wolfson EB, Holmes A, Gally DL, Holden NJ. 2015. Bacterial flagella: twist and stick, or dodge across the kingdoms. PLoS Pathog 11:e1004483. https://doi.org/10.1371/journal.ppat.1004483
- Kashefi K, Hartzell PL. 1995. Genetic suppression and phenotypic masking of a Myxococcus xanthus frzF- defect. Mol Microbiol 15:483–494. https://doi.org/10.1111/j.1365-2958.1995.tb02262.x
- Shrout JD, Tolker-Nielsen T, Givskov M, Parsek MR. 2011. The contribution of cell-cell signaling and motility to bacterial biofilm formation. MRS Bull 36:367–373. https://doi.org/10.1557/mrs.2011.67
- Li Y-H, Tian X. 2012. Quorum sensing and bacterial social interactions in biofilms. Sensors (Basel) 12:2519–2538. https://doi.org/10.3390/ s120302519

- Valentini M, Filloux A. 2016. Biofilms and cyclic di-GMP (C-di-GMP) signaling: lessons from *Pseudomonas aeruginosa* and other bacteria. J Biol Chem 291:12547–12555. https://doi.org/10.1074/jbc.R115.711507
- Hengge R, Pruteanu M, Stülke J, Tschowri N, Turgay K. 2023. Recent advances and perspectives in nucleotide second messenger signaling in bacteria. Microlife 4:uqad015. https://doi.org/10.1093/femsml/uqad015
- Jenal U, Reinders A, Lori C. 2017. Cyclic di-GMP: second messenger extraordinaire. Nat Rev Microbiol 15:271–284. https://doi.org/10.1038/ nrmicro.2016.190
- Römling U, Galperin MY, Gomelsky M. 2013. Cyclic di-GMP: the first 25 years of a universal bacterial second messenger. Microbiol Mol Biol Rev 77:1–52. https://doi.org/10.1128/MMBR.00043-12
- Hengge R. 2021. High-specificity local and global c-di-GMP signaling. Trends Microbiol 29:993–1003. https://doi.org/10.1016/j.tim.2021.02.003
- Paul K, Nieto V, Carlquist WC, Blair DF, Harshey RM. 2010. "The c-di-GMP binding protein YcgR controls flagellar motor direction and speed to affect chemotaxis by a "backstop brake" mechanism". Mol Cell 38:128– 139. https://doi.org/10.1016/j.molcel.2010.03.001
- Fang X, Gomelsky M. 2010. A post-translational, c-di-GMP-dependent mechanism regulating flagellar motility. Mol Microbiol 76:1295–1305. https://doi.org/10.1111/j.1365-2958.2010.07179.x
- Subramanian S, Gao X, Dann CE, Kearns DB. 2017. Moti (DgrA) acts as a molecular clutch on the flagellar stator protein mota in *Bacillus subtilis*. Proc Natl Acad Sci U S A 114:13537–13542. https://doi.org/10.1073/pnas. 1716231114

- Homma M, Kojima S. 2022. Roles of the second messenger c-di-GMP in bacteria: focusing on the topics of flagellar regulation and *Vibrio* spp. Genes Cells 27:157–172. https://doi.org/10.1111/gtc.12921
- Yang F, Xue D, Tian F, Hutchins W, Yang C-H, He C. 2019. Identification of c-di-GMP signaling components in *Xanthomonas oryzae* and their orthologs in xanthomonads involved in regulation of bacterial virulence expression. Front Microbiol 10:1402. https://doi.org/10.3389/fmicb.2019. 01402
- Steiner S, Lori C, Boehm A, Jenal U. 2013. Allosteric activation of exopolysaccharide synthesis through cyclic di-GMP-stimulated proteinprotein interaction. EMBO J 32:354–368. https://doi.org/10.1038/emboj. 2012.315
- Chang Y-W, Rettberg LA, Treuner-Lange A, Iwasa J, Søgaard-Andersen L, Jensen GJ. 2016. Architecture of the type IVa pilus machine. Science 351:aad2001. https://doi.org/10.1126/science.aad2001
- Shi W, Sun H. 2002. Type IV pilus-dependent motility and its possible role in bacterial pathogenesis. Infect Immun 70:1–4. https://doi.org/10.1128/ IAI.70.1.1-4.2002
- Ellison CK, Dalia TN, Vidal Ceballos A, Wang J-Y, Biais N, Brun YV, Dalia AB.
 Retraction of DNA-bound type IV competence pili initiates DNA uptake during natural transformation in *Vibrio Cholerae*. Nat Microbiol 3:773–780. https://doi.org/10.1038/s41564-018-0174-y
- Maier B, Wong GCL. 2015. How bacteria use type IV pili machinery on surfaces. Trends Microbiol 23:775–788. https://doi.org/10.1016/j.tim. 2015.09.002
- Craig L, Pique ME, Tainer JA. 2004. Type IV pilus structure and bacterial pathogenicity. Nat Rev Microbiol 2:363–378. https://doi.org/10.1038/ nrmicro885
- Pelicic V. 2008. Type IV pili: e pluribus unum? Mol Microbiol 68:827–837. https://doi.org/10.1111/j.1365-2958.2008.06197.x
- Merz AJ, So M, Sheetz MP. 2000. Pilus retraction powers bacterial twitching motility. Nature 407:98–102. https://doi.org/10.1038/ 35024105
- Skerker JM, Berg HC. 2001. Direct observation of extension and retraction of type IV pili. Proc Natl Acad Sci U S A 98:6901–6904. https:// doi.org/10.1073/pnas.121171698
- Wadhwa N, Berg HC. 2022. Bacterial motility: machinery and mechanisms. Nat Rev Microbiol 20:161–173. https://doi.org/10.1038/s41579-021-00626-4
- Yang Z, Li CY, Friedrich C, Sogaard-Andersen L. 2014. Type IV pili and exopolysaccharide-dependent motility in *Myxococcus xanthus*, p 183– 198. In Yang Z, PI Higgs (ed), Myxobacteria: genomics, cellular and molecular biology. Caister Academic Press, Norfolk, UK. https://doi.org/ 10.21775/9781910190616
- Zusman DR, Scott AE, Yang Z, Kirby JR. 2007. Chemosensory pathways, motility and development in *Myxococcus xanthus*. Nat Rev Microbiol 5:862–872. https://doi.org/10.1038/nrmicro1770
- Wall D, Kaiser D. 1999. Type IV pili and cell motility. Mol Microbiol 32:1– 10. https://doi.org/10.1046/i.1365-2958.1999.01339.x
- Spormann AM. 1999. Gliding motility in bacteria: insights from studies of Myxococcus xanthus. Microbiol Mol Biol Rev 63:621–641. https://doi.org/ 10.1128/MMBR.63.3.621-641.1999
- Black WP, Xu Q, Yang Z. 2006. Type IV pili function upstream of the Dif chemotaxis pathway in *Myxococcus xanthus* EPS regulation. Mol Microbiol 61:447–456. https://doi.org/10.1111/j.1365-2958.2006.05230.x
- Black WP, Yang Z. 2004. Myxococcus xanthus chemotaxis homologs DifD and DifG negatively regulate fibril polysaccharide production. J Bacteriol 186:1001–1008. https://doi.org/10.1128/JB.186.4.1001-1008.2004
- Moak PL, Black WP, Wallace RA, Li Z, Yang Z. 2015. The Hsp70-like StkA functions between T4P and Dif signaling proteins as a negative regulator of exopolysaccharide in *Myxococcus xanthus*. PeerJ 3:e747. https://doi.org/10.7717/peerj.747
- Pérez-Burgos M, García-Romero I, Jung J, Schander E, Valvano MA, Søgaard-Andersen L. 2020. Characterization of the exopolysaccharide biosynthesis pathway in *Myxococcus xanthus*. J Bacteriol 202:e00335-20. https://doi.org/10.1128/JB.00335-20
- Wallace RA, Black WP, Yang X, Yang Z. 2014. A CRISPR with roles in Myxococcus xanthus development and exopolysaccharide production. J Bacteriol 196:4036–4043. https://doi.org/10.1128/JB.02035-14

 Dye KJ, Yang Z. 2022. Analysis of Myxococcus xanthus vegetative biofilms with microtiter plates. Front Microbiol 13:894562. https://doi.org/10. 3389/fmicb.2022.894562

- Black WP, Wang L, Jing X, Saldaña RC, Li F, Scharf BE, Schubot FD, Yang Z.
 2017. The type IV pilus assembly ATPase PilB functions as a signaling protein to regulate exopolysaccharide production in *Myxococcus xanthus*. Sci Rep 7:7263. https://doi.org/10.1038/s41598-017-07594-x
- Skotnicka D, Petters T, Heering J, Hoppert M, Kaever V, Søgaard-Andersen L. 2016. Cyclic di-GMP regulates type IV pilus-dependent motility in *Myxococcus xanthus*. J Bacteriol 198:77–90. https://doi.org/10. 1128/JB.00281-15
- Petters T, Zhang X, Nesper J, Treuner-Lange A, Gomez-Santos N, Hoppert M, Jenal U, Søgaard-Andersen L. 2012. The orphan histidine protein kinase SgmT is a c-di-GMP receptor and regulates composition of the extracellular matrix together with the orphan DNA binding response regulator DigR in Myxococcus xanthus. Mol Microbiol 84:147–165. https://doi.org/10.1111/j.1365-2958.2012.08015.x
- Pogue CB, Zhou T, Nan B. 2018. PlpA, a PilZ-like protein, regulates directed motility of the bacterium *Myxococcus xanthus*. Mol Microbiol 107:214–228. https://doi.org/10.1111/mmi.13878
- Kuzmich S, Skotnicka D, Szadkowski D, Klos P, Pérez-Burgos M, Schander E, Schumacher D, Søgaard-Andersen L. 2021. Three PilZ domain proteins, PlpA, PixA, and PixB, have distinct functions in regulation of motility and development in *Myxococcus xanthus*. J Bacteriol 203:e0012621. https:// doi.org/10.1128/JB.00126-21
- Skotnicka D, Smaldone GT, Petters T, Trampari E, Liang J, Kaever V, Malone JG, Singer M, Søgaard-Andersen L. 2016. A minimal threshold of c-di-GMP is essential for fruiting body formation and sporulation in Myxococcus xanthus. PLoS Genet 12:e1006080. https://doi.org/10.1371/ journal.pgen.1006080
- Roelofs KG, Jones CJ, Helman SR, Shang X, Orr MW, Goodson JR, Galperin MY, Yildiz FH, Lee VT. 2015. Systematic identification of cyclic-di-GMP binding proteins in *Vibrio cholerae* reveals a novel class of cyclic-di-GMPbinding ATpases associated with type II secretion systems. PLoS Pathog 11:e1005232. https://doi.org/10.1371/journal.ppat.1005232
- Wang Y-C, Chin K-H, Tu Z-L, He J, Jones CJ, Sanchez DZ, Yildiz FH, Galperin MY, Chou S-H. 2016. Nucleotide binding by the widespread high-affinity cyclic di-GMP receptor MshE_N domain. Nat Commun 7:12481. https://doi.org/10.1038/ncomms12481
- Dye KJ, Yang ZM. 2020. Cyclic-di-GMP and ADP bind to separate domains of PilB as mutual allosteric effectors. Biochem J 477:213–226. https://doi.org/10.1042/BCJ20190809
- Niesen FH, Berglund H, Vedadi M. 2007. The use of differential scanning fluorimetry to detect ligand interactions that promote protein stability. Nat Protoc 2:2212–2221. https://doi.org/10.1038/nprot.2007.321
- Jumper J, Evans R, Pritzel A, Green T, Figurnov M, Ronneberger O, Tunyasuvunakool K, Bates R, Žídek A, Potapenko A, Bridgland A, Meyer C, Kohl SAA, Ballard AJ, Cowie A, Romera-Paredes B, Nikolov S, Jain R, Adler J, Back T, Petersen S, Reiman D, Clancy E, Zielinski M, Steinegger M, Pacholska M, Berghammer T, Bodenstein S, Silver D, Vinyals O, Senior AW, Kavukcuoglu K, Kohli P, Hassabis D. 2021. Highly accurate protein structure prediction with AlphaFold. Nature 596:583–589. https://doi. org/10.1038/s41586-021-03819-2
- Wu SS, Wu J, Kaiser D. 1997. The Myxococcus xanthus pilT locus is required for social gliding motility although Pili are still produceds. Mol Microbiol 23:109–121. https://doi.org/10.1046/j.1365-2958.1997. 1791550.x
- Hodgkin J, Kaiser D. 1979. Genetics of gliding motility in *Myxococcus xanthus* (myxobacterales): two gene systems control movement. Molec Gen Genet 171:177–191. https://doi.org/10.1007/BF00270004
- Li Y, Sun H, Ma X, Lu A, Lux R, Zusman D, Shi W. 2003. Extracellular polysaccharides mediate pilus retraction during social motility of *Myxococcus xanthus*. Proc Natl Acad Sci U S A 100:5443–5448. https://doi. org/10.1073/pnas.0836639100
- Yang Z, Ma X, Tong L, Kaplan HB, Shimkets LJ, Shi W. 2000. Myxococcus xanthus dif genes are required for biogenesis of cell surface fibrils essential for social gliding motility. J Bacteriol 182:5793–5798. https://doi.org/10.1128/JB.182.20.5793-5798.2000
- Dye KJ, Vogelaar NJ, Sobrado P, Yang Z. 2021. High-throughput screen for inhibitors of the type IV pilus assembly ATPase PilB. mSphere 6:e00129-21. https://doi.org/10.1128/mSphere.00129-21

Month XXXX Volume 0 Issue 0

- Dye KJ, Vogelaar NJ, O'Hara M, Sobrado P, Santos W, Carlier PR, Yang Z.
 2022. Discovery of two inhibitors of the type IV pilus assembly ATPase
 PilB as potential antivirulence compounds. Microbiol Spectr 10:e0387722. https://doi.org/10.1128/spectrum.03877-22
- Jelsbak L, Kaiser D. 2005. Regulating pilin expression reveals a threshold for S motility in *Myxococcus xanthus*. J Bacteriol 187:2105–2112. https:// doi.org/10.1128/JB.187.6.2105-2112.2005
- Xu Q, Black WP, Ward SM, Yang Z. 2005. Nitrate-dependent activation of the Dif signaling pathway of *Myxococcus xanthus* mediated by a NarX-DifA interspecies chimera. J Bacteriol 187:6410–6418. https://doi.org/10. 1128/JB.187.18.6410-6418.2005
- Zhou T, Nan B. 2017. Exopolysaccharides promote Myxococcus xanthus social motility by inhibiting cellular reversals. Mol Microbiol 103:729– 743. https://doi.org/10.1111/mmi.13585
- Hendrick WA, Orr MW, Murray SR, Lee VT, Melville SB, Henkin TM. 2017.
 Cyclic di-GMP binding by an assembly ATPase (PilB2) and control of type IV pilin polymerization in the gram-positive pathogen Clostridium perfringens. J Bacteriol 199. https://doi.org/10.1128/JB.00034-17
- Floyd KA, Lee CK, Xian W, Nametalla M, Valentine A, Crair B, Zhu S, Hughes HQ, Chlebek JL, Wu DC, Hwan Park J, Farhat AM, Lomba CJ, Ellison CK, Brun YV, Campos-Gomez J, Dalia AB, Liu J, Biais N, Wong GCL, Yildiz FH. 2020. C-di-GMP modulates type IV MSHA pilus retraction and surface attachment in Vibrio cholerae. Nat Commun 11:1549. https://doi. org/10.1038/s41467-020-15331-8
- 62. McMahon SG, Melville SB, Chen J. 2022. Mechanical limitation of bacterial motility mediated by growing cell chains. Biophys J 121:2461–2473. https://doi.org/10.1016/j.bpj.2022.05.012

- Jakovljevic V, Leonardy S, Hoppert M, Søgaard-Andersen L. 2008. PilB and PilT are ATPases acting antagonistically in type IV pilus function in Myxococcus xanthus. J Bacteriol 190:2411–2421. https://doi.org/10.1128/ JB.01793-07
- Campos JM, Geisselsoder J, Zusman DR. 1978. Isolation of bacteriophage MX4, a generalized transducing phage for *Myxococcus xanthus*. J Mol Biol 119:167–178. https://doi.org/10.1016/0022-2836(78)90431-x
- 65. Sukmana ABA. 2019. Understanding PilB, the type IV pilus assembly (T4P) ATPase. Blacksburg, VA Masters Virginia Tech
- Sukmana A, Yang Z. 2018. The type IV pilus assembly motor PilB is a robust hexameric ATPase with complex kinetics. Biochem J 475:1979– 1993. https://doi.org/10.1042/BCJ20180167
- Sun C, Li Y, Yates EA, Fernig DG. 2020. SimpleDSFviewer: a tool to analyze and view differential scanning fluorimetry data for characterizing protein thermal stability and interactions. Protein Sci 29:19–27. https:// doi.org/10.1002/pro.3703
- Schneider CA, Rasband WS, Eliceiri KW. 2012. NIH image to ImageJ: 25 years of image analysis. Nat Methods 9:671–675. https://doi.org/10. 1038/nmeth.2089
- Holm L, Laiho A, Törönen P, Salgado M. 2023. DALI shines a light on remote homologs: one hundred discoveries. Protein Sci 32:e4519. https://doi.org/10.1002/pro.4519
- Schrodinger, LLC. 2015. The PyMOL molecular graphics system, version 1.8. https://pymol.org/2/support.html#page-top.